

## Supporting Information

### Monitoring the interaction of a single G-protein key binding site with rhodopsin disk membranes upon light-activation

Tai-Yang Kim, Hiroshi Uji-i, Martina Moeller, Benoit Muls, Johan Hofkens, and Ulrike Alexiev

#### *Experimental procedures and data analysis*

##### *Sample preparation*

A variant of a high-affinity analogue (VLEDLKSCGLF (1)) from the C-terminal segment of the transducin  $\alpha$ -subunit, VLEDLKCVGLF (pG<sub>T</sub> $\alpha$ ), was synthesized at the Institute of Biochemistry, Universitaetsmedizin-Charite Berlin, and fluorescently labeled with Atto-647N-maleimide (Atto-Tec, Germany), yielding pG<sub>T</sub> $\alpha$ -F. Bovine retinæ were purchased from J. A. Lawson Corp (Lincoln, NE). Rod outer segment disk membranes were prepared from bovine retinæ and labeled with Atto-647N-maleimide at position C316 of rhodopsin essentially as described (2). Functional binding of pG<sub>T</sub> $\alpha$ -F was tested by the formation of additional Meta-II (Extra-Meta-II) in a concentration dependent manner at pH 8 and 3°C (Fig. S1a), as the pH and temperature dependent equilibrium between Meta-II and its precursor state is shifted towards Meta-II under these conditions (3). Flash spectroscopy was performed as described (2). The time constant for pG<sub>T</sub> $\alpha$ -F dissociation from light-activated disk membranes is 1-5 s as determined by double-time-resolved fluorescence spectroscopy (4).

For microscopy experiments layers of disk membranes were deposited at the surface of a glass cover slip in a buffer filled sample compartment. Individual Atto-647N labeled disk membranes are visible in the image presented in Figure S1c. The inset shows a fully covered glass surface, where individual membranes at the top layer are visible as brighter areas. For experiments with pG<sub>T</sub> $\alpha$ -F unlabeled

membranes were used. The Atto647N absorption band centered at  $651\pm 1$  nm (Fig. S1b, arrow 2) is well separated from the absorption band of rhodopsin with  $\lambda_{\max} = 498\pm 1$  nm (Fig. S1b, arrow 1). Thus, fluorescence excitation of pG<sub>T</sub>α-F at 633 nm (see below) should not result in accidental rhodopsin activation. The emission of pG<sub>T</sub>α-F with  $\lambda_{\max} = 666\pm 1$  nm is marked by arrow 3 (Fig. S1b).

### ***Fluorescence microscopy***

Wide-field fluorescence microscopy was performed using an inverted epi-fluorescence microscope (IX-71, Olympus) equipped with a cooled electron multiplying CCD camera (C9100-13, Hamamatsu). The fluorescently labeled rhodopsin disk membranes and pG<sub>T</sub>α-F were excited at 632.8 nm (He-Ne laser, Model 1145p, JDS Uniphase Co.). Light-activation of rhodopsin was carried out with a 2 ms light-pulse of 532 nm from a solid-state laser (CDPS532M-50, JDS Uniphase Co.) equipped with a mechanical shutter (Uniblitz-LS6, Vincent Associates). Both laser lines were circularly polarized using a 1/4 waveplate and directed onto the sample through the same dichroic mirror (Z633RDC, Chroma Technology, Inc.). The wide-field illumination was carried out in the TIRF (total internal reflection fluorescence) mode by focusing the expanded laser beams onto the back-focal plane of the objective (60x TIRF objective (PLAN APO, TIRF/NA1.45)). Only those pG<sub>T</sub>α-F molecules which interact with the membrane were visible. The emission of the fluorophore was collected with the same objective and imaged through the dichroic mirror and a long path filter (HQ655LP). The collected fluorescence image was further magnified 3.3x using a projection lens, resulting in a maximum view of  $41 \times 41 \mu\text{m}^2$  ( $80.8 \times 80.8 \text{ nm}^2$  / pixel). Movies were recorded with an integration time of 31 ms per frame (32 Hz). The photobleaching time constant of pG<sub>T</sub>α-F was  $\sim 10$  s under the experimental conditions.

### ***Data analysis***

Fluorescence images were analyzed using self-written routines in MATLAB (Mathworks). After filtering, background subtraction, and applying the triangle algorithm for thresholding, the signals originating from individual molecules in the original image were fitted to a two-dimensional Gaussian profile (5). The two-

dimensional trajectories of molecules interacting with the membrane were constructed from the correlated images of identical molecules in subsequent observations. Tests with simulated data showed that the positional accuracy was ~18 nm (analyzed according to reference 6,7). Additional simulations were performed to discriminate between immobilization and confined diffusion for the slow component (subpopulation 1). The upper bound of positional accuracy for low fluorescent molecules was ~21 nm, the lower bound for bright fluorescent molecules was ~15 nm. Bright and low fluorescent molecules were found within both subpopulations.

Individual trajectories were analyzed by determining the mean square displacement  $\langle r^2 \rangle$  as a function of elapsed time, where the lag time is  $t_{lag} = n\Delta t$  with  $n$  being the frame index and  $\Delta t$  denotes the frame interval. For the experiments presented in this study  $\Delta t = 31$  ms. The mean square displacement of a set of coordinates  $\{x_i, y_i\}$  was calculated as the average over all overlapping pairs

$$\langle r^2(t_{lag}) \rangle = \frac{1}{N-n} \sum_{i=1}^{N-n} [(x_{i+n} - x_i)^2 + (y_{i+n} - y_i)^2] \quad (1)$$

with  $N$  being the total number of frames in the trajectory. For a two-dimensional random diffusion the diffusion coefficient  $D$  is related to the mean square displacement  $\langle r^2 \rangle$  by

$$\langle r^2(t_{lag}) \rangle = 4Dt_{lag} \cdot \quad (2)$$

However, for non-homogeneous populations multiple diffusion coefficients can be introduced. This is better described by probability distribution functions (7-11). A characteristic radial probability distribution of displacements  $r$ ,  $p(r, t_{lag})$  for multiple subpopulations (8,9) is given by :

$$p(r, t_{lag}) dr = \sum_{i=1}^{N_D} A_i \frac{2}{4D_i t_{lag}} e^{-\frac{r^2}{4D_i t_{lag}}} r dr \quad (3)$$

with  $N_D$  being the number of subpopulations, and  $A_i$  the fractional amplitudes with the corresponding diffusion constants  $D_i$  and  $4D_i t_{lag} = r_i^2(t_{lag})$ .

Alternatively, a cumulative radial distribution function  $P(r, t_{lag})$  can be obtained by integration of  $p(r, t_{lag})$  over all  $r$ . For the case of  $P(r^2, t_{lag})$  and  $N_D=2$  the probability distribution is

$$P(r^2, t_{lag}) = 1 - \left( A \cdot e^{-\frac{r^2}{r_1^2}} + (1 - A) \cdot e^{-\frac{r^2}{r_2^2}} \right) \quad (4)$$

with  $A$  being the fractional amplitude (7).

For restricted diffusion, the confinement length  $L$ , i.e. diffusion within a square of side length  $L$ , and the initial diffusion constant  $D_0$  can be extracted from the data using (12):

$$r^2(t_{lag}) = \frac{L^2}{3} \left( 1 - \exp\left(-\frac{12D_0 t_{lag}}{L^2}\right) \right). \quad (5)$$

### ***Structure presentation***

The structure shown in Figure 1C (main text) was prepared with VMD (13).

### ***References***

- (1) Martin, E.L., Rens-Domiano, S., Schatz, P.J., Hamm, H.E. (1996) Potent peptide analogues of a G protein receptor-binding region obtained with a combinatorial library. *J.Biol. Chem.* 271, 363-366.
- (2) Alexiev, U., Rimke, I., and Pöhlmann, T. (2003) Elucidation of the Nature of the Conformational Changes of the EF-interhelical loop in bacteriorhodopsin and of the helix VIII on the cytoplasmic surface of bovine rhodopsin: a time-resolved fluorescence depolarization study. *J. Mol. Biol.* 328, 705-719.
- (3) Kisselev, O.G., Meyer C.K., Heck, M., Ernst O.P. and Hofmann, K.P. (1999) Signal transfer from rhodopsin to the G-protein: evidence for a two-site sequential fit mechanism. *Proc. Natl.*

- (4) Kim, T.Y., Winkler, K. and Alexiev, U. (2007) Picosecond multidimensional fluorescence spectroscopy: A tool to measure real-time protein dynamics during function. *Photochem. Photobiol.* 83, 378-384.
- (5) Rocha S, Hutchison JA, Peneva K, Herrmann A, Müllen K, Skjøt M, Jørgensen CI, Svendsen A, De Schryver FC, Hofkens J, Uji-I H. Linking Phospholipase Mobility to Activity by Single-Molecule Wide-Field Microscopy. (2009) *Chemphyschem.* 10,151-161.
- (6) Bobroff, N. (1986) Position measurements with a resolution and noise-limited instrument. *Rev. Sci. Instr.* 57, 1152-1157
- (7) Schütz, G.J., Schindler, H., Schmidt, T., *Biophys J.* (1997) Single-molecule microscopy on model membranes reveals anomalous diffusion. *Biophys. J.* 73, 1073-80
- (8) Anderson, C.M., Georgiou, G.N., Morrison, I.E., Stevenson, G.V., and Cherry, R.J. (1992) Tracking of cell surface receptors by fluorescence digital imaging microscopy using a charge-coupled device camera. Low-density lipoprotein and influenza virus receptor mobility at 4 degrees C. *J. Cell. Sci.* 101, 415-425
- (9) Kues, T., Dickmanns, A., Lührmann, R., Peters, R., Kubitscheck, U. (2001) High intranuclear mobility and dynamic clustering of the splicing factor U1 snRNP observed by single particle tracking. *Proc. Natl. Acad. Sci. U S A.* 98, 12021-12026.
- (10) Vrljic, M., Nishimura, S.Y., Brasselet, S., Moerner, W.E., McConnell, H.M. (2002) Translational diffusion of individual class II MHC membrane proteins in cells. *Biophys. J.* 83, 2681-2692
- (11) Chandrasekar, S. (1943) Stochastic problems in physics and astronomy. *Rev. Mod. Phys.* 15, 1-89
- (12) Kusumi, A., Sako, Y., Yamamoto, M. (1993) Confined lateral diffusion of membrane receptors as studied by single particle tracking (nanovid microscopy). Effects of calcium-induced differentiation in cultured epithelial cells. *Biophys. J.* 65, 2021-2040.
- (13) Humphrey, W., Dalke, A., and Schulten, K. (1996) VMD: visual molecular dynamics. *J. Mol. Graph.* 14(1), 33-38, 27-38

## Figures

### Figure S1

a) Extra-Meta-II formation at different concentrations of pG<sub>T</sub>α-F.

Inset: Half maximum concentration of pG<sub>T</sub>α-F for the formation of Extra-Meta-II. The binding affinity of pG<sub>T</sub>α-F is in the same range as the parent peptide (HAA) (3).

b) Absorption spectra of rhodopsin (arrow 1) and pG<sub>T</sub>α-F (arrow 2) and emission spectrum of pG<sub>T</sub>α-F (arrow 3).

c) Fluorescence image to visualize individual rhodopsin membranes. Scale bar: 2 μm. Inset: Glass surface fully covered with layers of rhodopsin membranes.

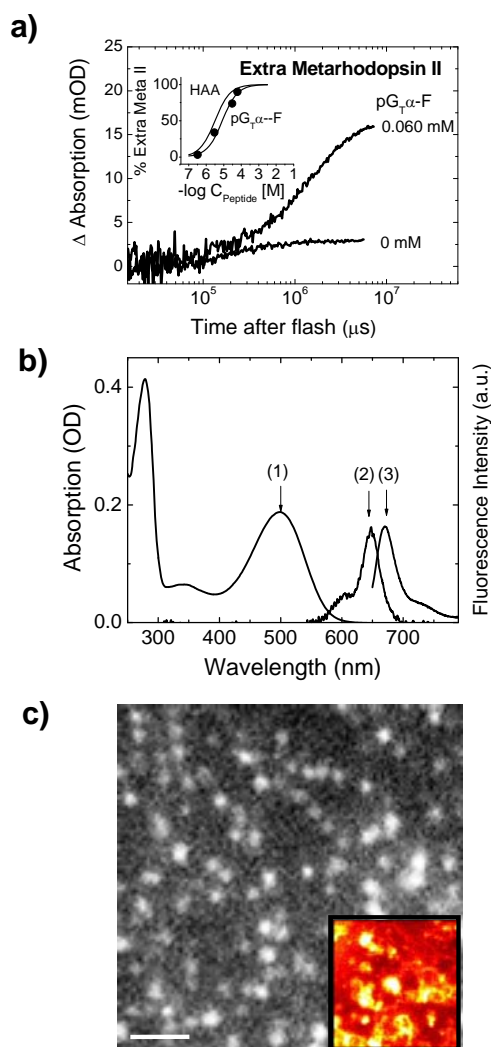


## Figure S2

Control of instrument drift. Drift analysis on experimental data shows no indication for a systematic drift. Lines indicate particle movement (100x amplified) integrated over 310ms (10 frames). 5 consecutive groups are shown in different colors. A given color shows displacements occurring simultaneously.

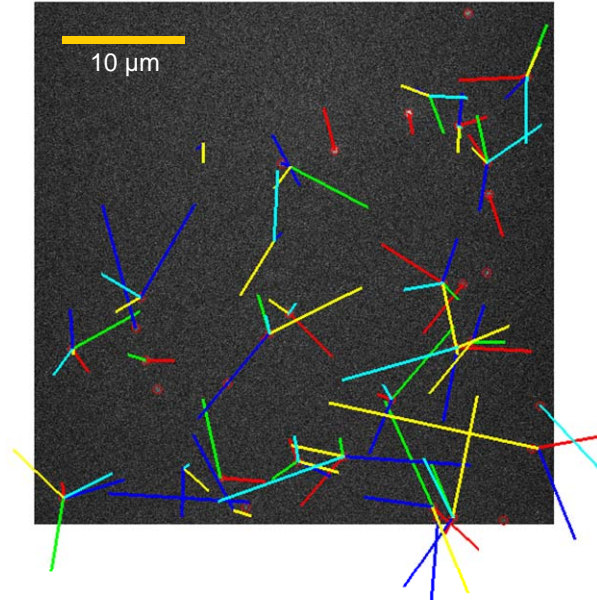


## Figure S3

Residence times.

- Residence time histogram of 2517 pG<sub>T</sub>α-F molecules interacting with dark rhodopsin membranes.
- Residence time histogram of 614 pG<sub>T</sub>α-F molecules interacting with light-activated rhodopsin membranes.

